Site-Specific Delivery of Oligonucleotides to Hepatocytes after Systemic Administration

ARTICLE *in* BIOCONJUGATE CHEMISTRY · FEBRUARY 2008

Impact Factor: 4.51 · DOI: 10.1021/bc070126m · Source: PubMed

5 AUTHORS, INCLUDING:

Zhaoyang Ye
East China University of Science and Technol…
47 PUBLICATIONS **572** CITATIONS
SEE PROFILE

Kun Cheng
University of Missouri - Kansas City
31 PUBLICATIONS **784** CITATIONS
SEE PROFILE

Duane D Miller
University of Tennessee
436 PUBLICATIONS **7,831** CITATIONS
SEE PROFILE

Ram I Mahato
University of Nebraska Medical Center
147 PUBLICATIONS **5,009** CITATIONS
SEE PROFILE

Published in final edited form as:
Bioconjug Chem. 2008 January ; 19(1): 290–298. doi:10.1021/bc070126m.

Site-specific Delivery of Oligonucleotides to Hepatocytes after Systemic Administration

Lin Zhu, **Zhaoyang Ye**, **Kun Cheng**, **Duane D. Miller**, and **Ram I. Mahato***
Department of Pharmaceutical Sciences University of Tennessee Health Science Center, Memphis, TN 38163, USA

Abstract

We previously complexed ODN with galactosylated poly (L-lysine) (Gal-PLL) to enhance its site specific delivery to hepatocytes. To avoid the use of polycations, in this study we conjugated galactosylated poly (ethylene glycol) (Gal-PEG (MW of PEG: 3486±500Da)) to ODN via an acid labile ester linkage of *β*–thiopropionate. Following tail vein injection into rats, Gal-PEG-^{33}P-ODN rapidly cleared from the circulation and 60.2% of the injected dose accumulated in the liver at 30 min post injection, which was significantly higher than that deposited after injection of ^{33}P-ODNs. The plasma concentration versus time profile of Gal-PEG-^{33}P-ODN was biphasic, with 4.38±0.36 min as $t_{1/2}$ of distribution and 118.61±22.06 min as $t_{1/2}$ of elimination. Prior administration of excess Gal-BSA decreased the hepatic uptake of Gal-PEG-^{33}P-ODN from 60.2% to 35.9%, suggesting galactose triggers the asialoglycoprotein receptor-mediated endocytosis of Gal-PEG-^{33}P-ODN by hepatocytes. A large proportion of the injected Gal-PEG-^{33}P-ODN was taken up by the hepatocytes as evidence by determination of radioactivity in the digested liver cells upon liver perfusion and separation by centrifugation on a Nycodenz gradient. In conclusion, Gal-PEG-ODN conjugate may be used for treating a variety of liver diseases.

Keywords

Oligonucleotides; conjugate; biodistribution; hepatocytes; site-specific delivery

INTRODUCTION

Oligonucleotides (ODNs) have attracted much attention as a new class of therapeutic agents that can be used for gene modulation. However, in vivo gene silencing by ODNs has not yet been successful because of several obstacles, including the nonspecific interaction with plasma proteins, wide distribution and poor stability against enzymatic degradation. Since phosphodiester ODNs have extremely short half-lives due to degradation by nucleases, phosphorothioate (PS) ODNs are commonly used. PS ODNs are fairly stable *in vivo*, but readily bind to serum proteins, leading to undesirable biological events. To address these problems, a variety of delivery systems composed of cationic lipids (1–3) and cationic polymers (4–6) have been developed. Some of these delivery systems substantially enhanced the enzymatic stability and uptake into the target cells in vitro (7). However, most of these cationic carriers are inefficient in vivo because of their non-specific biodistribution in the body.

We and others have shown that ODNs are cleared rapidly from the circulation and accumulated to most of the peripheral tissues, with the highest accumulation in the liver and kidney (8–

* Corresponding authors: Ram I. Mahato, Ph.D. 19 Manassas, Room 224, Memphis, TN 38163, USA, Tel: (901) 448-6929, Fax: (901) 448-6092, E-mail: rmahato@utmem.edu, http://cop.utmem.edu/rmahato.

12). The asialoglycoprotein receptor is located on parenchymal liver cells (e.g., hepatocytes) and recognizes terminal galactose (13) or lactose residues (14,15). Therefore, we previously used galactosylated poly (L-lysine) (Gal-PLL) for complex formation with ODNs and demonstrated enhanced hepatic uptake of ODNs, which was influenced by the particle size, zeta potential, sugar substitution, and molecular weight of both polycations and ODNs (16). Although the uptake of Gal-PLL/ODN complexes by hepatocytes was significantly higher than that of naked ODNs, the difference of their distribution to different liver cells was only moderate. To avoid the use of polycations, Rajur et al. (1997) covalently conjugated ODNs to asialoorosomucoid via a disulfide bond using sulfosuccinimidyl 6-[3′-(2-pyridyldithio) propionamido] hexanoate (sulfo-LC-SPDP), but the authors did not test the conjugate *in vivo* (17).

PEGylation is known to significantly enhance the ODN stability against exonucleases and reduce renal clearance compared to unmodified ODNs (18). The in vivo activity of a drug depends in part on its rate of excretion and degradation. PEGylation should promote the bioactivity of an ODN by increasing plasma residence time and decreasing nuclease degradation. PEGylation also shield the inherent negative charge of the ODN, thereby possibly facilitating cellular uptake of the conjugated drug. Additionally, PEGylation could potentially diminish the immunostimulatory effects of the ODNs (19,20). Keeping these benefits in mind, Bonora etal. (1997) conjugated ODNs to poly(ethylene glycol) (PEG) through a covalent linkage (21). However, these PEG-ODN conjugates were less effective, since PEG could not be cleaved early from the ODNs in the cytoplasm. Therefore, Oishi et al. conjugated ODN to acrylated or lactosylated PEG through a pH-responsive ester (22,23). However, these authors did not determine the biodistribution of Lac-PEG-ODN and used in conjunction with a cationic polymer like linear polyethyleneimine (PEI), which is likely to promote non-specific interaction with plasma proteins and uptake by phagocytic cells.

In this study, we used fully phosphorothioate G-rich ODN, which is fairly stable, but binds to serum proteins (24). To minimize binding to plasma proteins, enhance stability and prolong circulation time, we conjugated Gal-PEG to ODN using an acid labile linker. Gal-PEG is expected to enhance ODN delivery to the hepatocytes whose inflammation and injury lead to progression of liver fibrosis (25). In this study, we conjugated ODN to Gal-PEG via an acid labile ester linkage and used without any cationic polymers or lipids to avoid cytotoxicity and non-specific interaction. Following conjugation and in vitro characterization, we determined the biodistribution of Gal-PEG-^{33}P-ODN at whole body, organ (liver) and cellular (liver cells) levels after tail vein injection into rats.

MATERIALS AND METHODS

Materials

25 mer ODN (5′ GAG GGG GGA GGA GGG AAA GGA AGG G 3′) modified with a sulfhydryl group at the 3′ end was purchased from Invitrogen Corporation (Carlsbad, CA). [γ-^{33}P]ATP was obtained from MP Biomedicals (Irvine, CA) and T4 polynucleotide kinase (T4-PNK) from New England Biolabs (Beverly, MA). Bio-Gel P-6DG gel from Bio-Rad Laboratories (Hercules, CA). PD-10 desalting columns were obtained from Pharmacia Fine Chemicals AB (Uppsala, Sweden). Soluene®-350 (tissue solubilizer) and Hionic-Fluor (scintillation fluid) were purchased from Perkin Elmer (Boston, MA). Isoflurane was obtained from Baxter Health Corporation (Deerfield, IL). Type IV collagenase was purchased from Worthington Biochemical Corporation (Lakewood, NJ). Nycodenz™ AG was obtained from Greiner Bio-One Inc. (Longwood, FL). PE-60 polyethylene tube was purchased from Becton Dickinson and Company (Sparks, MD) and heparin solution was procured from American Pharmaceutical Partners, Inc. (Los Angeles, CA). Acrylate-PEG-NHS (MW: 3486±500Da) was purchased from Nektar Therapeutics (Huntsville, AL). Bovine serum albumin (BSA)

(fraction V, purity >98%) was purchased from USB Corporation (Cleveland, OH). Palladium (10 wt % on activated carbon), thiophosgene, Brilliant Blue R Staining Solution, dithiothreitol (DTT), p-nitrophenyl β-D-galactopyranoside, Dimethylformamide (DMF), 2,5- Dihydroxy benzoic acid (DHB), methylene blue, deuterium oxide (D_2O), triethylamine (TEA, HPLC grade), and pronase were purchased from Sigma-Aldrich Chemicals Limited (St. Louis, MO). Dialysis tubing (MWCO 1,000 Da) was purchased from Spectrum Laboratories, Inc. (Houston, TX). Amicon Centricon filter devices (MWCO 10,000 Da) were purchased from Millipore Corporation. (Billerica, MA). Hydrogen peroxide (H_2O_2), acetic acid, acetonitrile (ACN, HPLC grade) and water (HPLC grade) were purchased from Fisher Chemical (Fair Lawn, NJ). Ca^{2+}/Mg^{2+}-free Hank's balanced salt solution (Cellgro) was purchased from Media Tech (Washington, DC).

Animals

Male Sprague-Dawley rats weighing 140–160 g were purchased from Harlan Co. (San Diego, CA) and were housed individually under the controlled light (12/12h) and temperature conditions and had free access to food and water.

Synthesis of Gal-PEG-ODN Conjugate

p-Nitrophenyl β-D-galactopyranoside (200 mg) was reduced with 200 mg of 10% palladium on activated carbon under hydrogen (1 atm) in 30 ml of a 1:1 (v/v) ethanol-water mixture for 2h, as described by Monsigny et al (26). The product, p-aminophenyl β-D-galactopyranoside, was concentrated by solvent removal under vacuum and characterized using ^1H NMR and mass spectrometry after dissolving in D_2O, and the NMR spectra were recorded on a Bruker ARX-300 MHz spectrometer at 25 °C. Chemical shifts were recorded in ppm relative to D_2O (δ 4.79, 1H). Electron spray ionization (ESI) mass spectra were obtained after dissolving the product in methanol on an ESQUIRE-LC Ion Trap LC/MS system. Acrylate polyethylene glycol N-hydroxysuccinimidyl (NHS) ester (acrylate-PEG-NHS) (58mg) and *p*-aminophenyl *β*-D-galactopyranoside (43.4 mg) were dissolved separately in 0.4ml of DMF, mixed together, and dialyzed in 500ml water for 48h with MWCO 1,000. The product, galactose (Gal)-PEG-acrylate was characterized by ^1H NMR after dissolving the product in D_2O. The molecular weight of Gal-PEG-ODN was determined using Matrix Assisted Laser Desorption/Ionization Time-of-Flight (MALDI-TOF) mass spectrometry with DHB as a matrix.

Modified ODNs were treated with 0.2M dithiothreitol (DTT) in 0.1M, pH 9.0 glycine buffer containing 0.1M NaCl for 3h at room temperature to generate a 3′-thiol functional group. Excess DTT was removed by extraction with ethyl acetate, and ODN was precipitated by adding 2.6 volume of ethanol after addition of sodium acetate (NaOAc) to 0.3M. The mixture was kept at −30°C overnight and centrifuged at 13000g for 30min. The ODN with 3′-thiol functional group and Gal-PEG-acrylate were dissolved in 0.4mL water at a molar ratio of 1:100, stirred under nitrogen protection at room temperature for 6h, and then centrifuged the mixture by Amicon Centricon filter device (MWCO 10,000 Da) at 2, 500g for 30min. The upper solution of the filter device was collected and lyophilized. The formation of Gal-PEG-ODN was verified on 20% native polyacrylamide gel electrophoresis at 8V/cm for 100min at room temperature, followed by gel staining with methylene blue. The reaction mixtures and the purity of intermediate and final products were monitored by Reverse Phase-High Performance Liquid Chromatography (RP-HPLC), which was carried on a reverse phase C18 column (250mm×4.6mm, Alltech, Deerfield, IL) by an HPLC system (Waters, Milford, MA) with detection at 260nm using a gradient of 5% – 80% ACN in 0.1M triethylammonium acetate at a flow rate of 1.0mL/min at 56ºC.

Synthesis of Galactosylated Albumin

Gal-BSA was synthesized from p-aminophenyl β-D-galactopyranoside and BSA (MW 66000Da) using a modified method described by Sando and Karson (27). After conjugation Gal-BSA was purified by PD-10 column and identified by sodium dodecyl sulfate polyacrylamide gel electrophoresis (SDS-PAGE) followed by staining with Brilliant Blue R Staining Solution. The molar ratio of galactose and BSA was about 15. Sugar (galactose) content was determined by the resorcinol-sulfuric acid method as described by Monsigny et al (28).

Radiolabeling of Oligonucleotides

The 25 mer ODN or Gal-PEG-ODN was labeled by adding γ-^{33}P to the 5′ end using [γ-^{33}P] ATP and T4-PNK, using the manufacturer's protocol. Briefly, 1μg of ODN or Gal-PEG-ODN was mixed with 5μl of T4-PNK buffer, 2μl of T4-PNK, and 4μl of [γ-^{33}P] ATP. The reaction mixture was incubated at 37°C for 60min, followed by incubation at 70°C for 10min to stop the reaction. Unincorporated [γ-^{33}P] ATP was removed from radiolabeled ODN or Gal-PEG-ODN by size exclusion chromatography with Bio-Gel P-6DG gel. Radioactivity was measured on TRI-CARB®2000 liquid scintillation analyzer (PACKARD Instrument Company, Meridon, CT). The incorporation efficiency of the purified ^{33}P-ODN was determined by trichloroacetic acid (TCA) precipitation method and the value was more than 95%. The specific activity of ^{33}P-ODN was about 5×10^5~10×10^5 cpm/μg.

Dissociation and Stability

To determine whether ODNs can dissociate from Gal-PEG-ODN conjugate after endocytosis, this conjugate was incubated at 37ºC in Tris HCl buffer of pH 5.5 for 1, 2 and 4h. In addition we also incubated this conjugate in the rat serum at 37ºC to determine its stability. These samples were then detected by 20% polyacrylamide gel electrophoresis and autoradiography.

Biodistribution of Gal-PEG-ODN

The animal protocol was approved by the Animal Care and Use Committee (ACUC), Department of Comparative Medicine, University of Tennessee Health Science Center, Memphis, TN 38163. Male Sprague-Dawley rats weighing 140–160g were used in this study and 4 rats were used for each time point. Unlabeled and Gal-PEG-^{33}P-ODN were mixed in saline to give a final concentration of 1mg/ml and specific activity of 1×10^6 cpm/ml. Rats were anesthetized by inhalation of isoflurane and Gal-PEG-^{33}P-ODN or ^{33}P-ODN was injected via tail vein at a dose of 0.2mg/Kg body weight. At 2.5, 5, 15, 30, 90, 240 and 1440 min post injection, 0.5ml blood was collected by cardiac puncture in heparinized tubes, and urine was collected directly from the bladder using 0.26 gauge needle syringe. The animals were then sacrificed and major tissues (liver, kidney, spleen, heart, lung and muscle) were collected, washed, blotted dry, weighed and stored at −80ºC. The radioactivity of urine sample was counted directly after adding 10 ml of scintillation fluid. Two hundred microliters of plasma and 200mg of each tissue were incubated with 2ml tissue solubilizer for 3h at 55°C and overnight at 37°C in shaker. Four hundred microliters of H_2O_2 was added and incubated at 55° C for another 30 min. Ten milliliters of scintillation fluid was added to each sample and the radioactivity was counted using a liquid scintillation counter.

Determination of Pharmacokinetic Profiles

Plasma data was analyzed using WinNonlin Professional (version 5.0.1, Pharsight Corporation, Mountainview, CA). The Gal-PEG-^{33}P-ODN plasma concentration data versus time were fitted using one- and two-compartment models, and pharmacokinetic parameters were calculated area under the curve (AUC), C_{max}, T_{max} and Clearance (CL).

The data were best fitted to a two compartment model where

$$C_t = Ae^{-\alpha t} + Be^{-\beta t} \quad (1)$$

and C_t equals concentration at time t, A and B are the y-axis intercepts, and α and β are the hybrid constants for distribution and elimination, respectively. Tissue distribution data of Gal-PEG-^{33}P-ODN were analyzed in terms of clearance and tissue uptake rate index using biexponential equations as described previously (8). The change in the amount of radioactivity in a tissue with time can be described as follows:

$$dT(t)/t = CL_{in}C(t) - K_{out}T(t) \quad (2)$$

where T(t) (% of dose/g) represents the amount of radioactivity in 1 g of the tissue, C(t) (% of dose/mL) is the plasma concentration of radioactivity, CL_{in} ($mLh^{-1}g^{-1}$) is the tissue uptake rate index from the plasma to the tissue, and K_{out} (h^{-1}) is the rate constant for efflux from the tissue. In the present study, the efflux process can be considered negligible during the initial time points up to 90 min. Hence, eq 1 integrates to

$$CL_{in} = T(t_1)\int_0^{t_1} C(t_1)dt = T(t_1)/AUC_{0-t_1} \quad (3)$$

where t_1 (h) is the sampling time. According to eq 2, the tissue uptake rate index is calculated using the amount of radioactivity in the tissue and the area under the plasma concentration-time curve (AUC). Then, the organ clearance (CL_{org}) is expressed as follows:

$$CL_{org} = CL_{in}W \quad (4)$$

where W (g) is the total weight of the organ. When the tissue uptake process followed nonlinear kinetics, CL_{in} values would represent an average value for the overall experimental period. Total body clearance (CL_{total}) was calculated from AUC for infinite time (AUC_∞) by the following equation:

$$CL_{total} = dose/AUC_\infty \quad (5)$$

The tissue uptake clearance and index were calculated using the values up to 30 min after injection, assuming that ODNs were fairly stable within this period.

Competition in Hepatic Uptake of Gal-PEG-ODN

Two minutes before the injection of Gal-PEG-^{33}P-ODN at a dose of 0.2mg/kg (specific activity: 1×10^6cpm/mL), rats received 10mg/Kg of Gal-BSA via tail vein injection. At 30 min post injection, blood and urine were collected; other major organs were harvested as described above for radioactive measurement.

Hepatic Cellular Distribution of Gal-PEG-ODN

To determine the effect of conjugation with Gal-PEG on the hepatic uptake of ODNs, the liver was isolated and perfused in situ with Ca^{2+}/Mg^{2+}- free Hanks' balanced salt solution containing 0.1% pronase and 0.05% collagenase at 30 min post intravenous injection of ^{33}P-ODN or Gal-PEG-^{33}P-ODN into rats as described previously (24). Briefly, rats (200–250g) were anesthetized by inhalation of isoflurane, and 100 IU of heparin was injected via tail vein, the abdomen was opened, and the portal vein was cannulated with PE-60 polyethylene tube. The liver was pre-perfused with 2ml diluted heparin solution, then with 200 ml Ca^{2+}/Mg^{2+}-free Hank's balanced salt solution and finally with Hank's balanced salt solution containing 0.05% type IV collagenase and 0.1% pronase for additional 250 ml. All the perfusion solutions were incubated at 37°C. After perfusion, different liver cell types were separated by Nycodenz

gradient (29) and radioactivity was measured. The contributions of various cell types to the total liver uptake were calculated as percentage of total hepatic uptake.

Statistical Analysis

Data were expressed as the mean ± standard deviation (SD). The difference between any two groups was determined by ANOVA. $P<0.05$ was considered statistically significant.

RESULTS

Chronic injury and inflammation of hepatocytes often lead to liver fibrosis and loss of sinusoidal fenestrae, suggesting that liposomal and nanoparticulate delivery systems may not be good for ODN delivery to the hepatocytes. Therefore, we synthesized Gal-PEG and conjugated to ODN by *β*–thiopropionate, an acid-labile linkage which is easily cleaved at acidic pH, leading to endosomal release of ODNs after endocytosis (23). Following synthesis and characterization, we determined the biodistribution at whole body, organ (liver) and cellular (liver cells) levels after systemic administration of Gal-PEG-^{33}P-ODN in rats.

Synthesis and Characterization of Gal-PEG-acrylate and Gal-PEG-ODN

The synthesis scheme of Gal-PEG-ODN conjugate is shown in Figure 1. P-nitrophenyl *β*-D-galactopyranoside was reduced to p-aminophenyl *β*-D-galactopyranoside. ESI-MS and ^{1}H NMR results of this intermediate product are shown in Figure 2. ESI-MS (positive ion mode): 294.1 ($[M + Na]^+$) (Figure 2A); ^{1}H NMR (D_2O): δ 6.73 (d, 1H), 6.90 (d, 1H), 5.35 (s, 1H), 3.76–4.09 (m, 4H), 3.61 (m, 2H) (Figure 2B). Gal-PEG-acrylate was synthesized from NHS-PEG-acrylate and identified by MALDI-TOF MS and ^{1}H NMR. For MALDI-TOF MS, DHB was used as a matrix at the weight ratio of 1:2 (Gal-PEG-acrylate/DHB). Molecular weight of Gal-PEG-acrylate was 3758Da after conjugation between acrylate-PEG-NHS (MW 3486Da) and p-aminophenyl β-D-galactopyranoside (MW 271Da) (Figure 3A). ^{1}H NMR (D_2O): δ 7.35 (d, 2H), 7.12 (d, 2H), 5.54 (s, 1H), 3.48–3.92 (m, 538H), 5.93 (d, 2H), 6.17(t, 1H), 6.40 (d, 1H) (Figure 3B). Gal-PEG was then conjugated to ODN by Michael addition from p-aminophenyl β-D-galactopyranoside and Gal-PEG-acrylate. Gal-PEG-ODN was also identified by native polyacrylamide gel electrophoresis and staining with methylene blue (Figure 4). For the purification process, the RP-HPLC was used to monitor the mixtures and the purity of the intermediate and final products. From the HPLC chromatograms of ODNs, PEG and Gal-PEG-ODN conjugate shown in Figure 5, almost all PEG and ODNs were removed from the conjugate after purification. G-rich ODNs used in this study has the tendency to form G-quartets, which may decrease the recovery of the conjugate.

Dissociation and Stability

To determine the dissociation and stability of Gal-PEG-^{33}P-ODN, the radioactivity of the samples was measured after gel electrophoresis and autoradiography at 0, 1, 2 and 4 h post-incubation of the conjugate in Tris HCl buffer of pH 5.5 and rat serum, respectively. In the pH 5.5 buffer, the band of Gal-PEG-^{33}P-ODN gradually disappeared along the incubation time, while the band of the ^{33}P-ODN was still there even up to 4h (Figure 6). In contrast, this conjugate was fairly stable in rat serum for at least 4 h. The result suggests that the conjugate was fairly stable in serum, but its acid labile ester linkage can be cleaved at acidic pH. Our study also confirmed the previous report about this kind of conjugates by Oishi et al (23).

Biodistribution of Gal-PEG-ODN Conjugate

Following synthesis and purification of Gal-PEG and then conjugation to ^{33}P-ODN, we determined the biodistribution of Gal-PEG-^{33}P-ODN at 2.5, 5, 15, 30, 90, 240 and 1440 min post injection into the tail vein of rats. Figure 7A shows the time course of radioactivity in the

plasma, urine, liver, kidney, lung, heart and spleen (radioactivity in muscle was too low, not shown here). Gal-PEG-^{33}P-ODN was rapidly cleared from the circulation with less than 10% of radioactivity detected in the plasma at 30min post-injection. Correspondingly hepatic uptake of Gal-PEG-^{33}P-ODN increased with time and reached its peak at 30min post administration and then decreased with time. To compare the biodistribution profiles of Gal-PEG-^{33}P-ODN, ^{33}P-ODN was also injected into rats, and ODN accumulation and concentration in different organs were determined at 30min post-injection. Figure 7B shows the tissue concentration of Gal-PEG-^{33}P-ODN in the plasma (μg/mL) and tissues (μg/g) after tail vein injection into rats, while the conjugation of ODN with Gal-PEG significantly increased the accumulation of radioactivity (% of dose) in the liver, as compared to that of ^{33}P-ODN. Gal-PEG-^{33}P-ODN concentration was high not only in the liver, but also in the spleen and kidney (Figure 7). Almost 60.2% (about 2.88 μg ODN/g liver tissue) of the conjugate accumulated in the liver compared to about 40% (data not shown) (about 2.01 μg ODN/g liver tissue) accumulation by free ODNs at 30min post administration.

Plasma elimination of Gal-PEG-^{33}PODN was biphasic with a distribution half-life ($t_{1/2\alpha}$) of 4.38±0.36 min and elimination half-life ($t_{1/2\beta}$) of 118.61±22.06 min. Figure 8 summarizes the pharmacokinetic parameters such as AUC, V_d, CL and MRT. Consistent with rapid clearance (0.37±0.09 ml/min), Gal-PEG-^{33}P-ODN had a large V_d of 35.98±2.64 ml. Table 1 summarizes the AUC, tissue uptake rate index and organ clearance for representative organs after systemic administration of ^{33}P-ODN and Gal-PEG-^{33}P-ODN in rats. The liver uptake rate index and clearance of Gal-PEG-^{33}P-ODN were significantly higher than those of ^{33}P-ODN: 2663.27 ± 56.63 versus 376.15 ± 38.34 $\mu L \cdot h^{-1} \cdot g^{-1}$ and 16674.22±354.55 versus 2218.09± 205.68 $\mu L \cdot h^{-1} \cdot g^{-1}$, respectively. The spleen was in the second place with the tissue uptake rate index of 969.26 ± 51.79 versus 204.73 ± 9.64 $\mu L \cdot h^{-1} \cdot g^{-1}$ and CL_{org} of 395.84±21.15 versus 82.85 ± 7.32 $\mu L \cdot h^{-1}$. The tissue uptake rate indices and organ clearances of heart, kidney and lung were significantly higher than those of ^{33}P-ODN, possibly due to increased in vivo stability of ODN upon conjugation with Gal-PEG.

Competition in Hepatic Uptake of Gal-PEG-^{33}P-ODN

The role of asialoglycoprotein receptor on biodistribution of Gal-PEG-^{33}P-ODN in rats was assessed by determining the effect of excess Gal-BSA on the accumulation of Gal-PEG-^{33}P-ODN in the liver. Galactosylated proteins or polymeric systems are known to be taken up by asialoglycoprotein receptor-mediated endocytosis. We have previously demonstrated that one minute pre-injection of excess Gal-BSA can saturate asialoglycoprotein receptors present on the surface of hepatocytes, resulting in decreased hepatic uptake of Gal-PLL/ODN complexes. Staud et al. (1999) also injected galactosylated superoxide dismutase (Gal-SOD) two minute post-injection of excess Gal-BSA and demonstrated significant decrease in the hepatic uptake of Gal-SOD (13). Therefore, 2min interval between the intravenous injections of Gal-BSA and Gal-PEG-ODN is reasonable for the competition study. Systemic administration of excess Gal-BSA is known to saturate the asialoglycoprotein receptor of the hepatocytes (30). Prior administration of Gal-BSA at a dose of 10mg/Kg caused a significant decrease in the hepatic uptake of Gal-PEG-^{33}P-ODN, but increase in the radioactivity in plasma and other organs at 30 min post injection. The hepatic uptake of Gal-PEG-^{33}P-ODN decreased from 60.2% to 35.9% (Figure 9). This suggests the involvement of asialoglycoprotein receptor in their hepatic uptake.

Hepatic Cellular Localization

To determine the intrahepatic localization of Gal-PEG-^{33}P-ODN and to determine whether the uptake of this conjugate by hepatocytes is mediated by asialoglycoprotein receptors, the liver was perfused at 30min post tail vein injection of ^{33}P-ODN or Gal-PEG-^{33}P-ODN, and different types of liver cells were isolated for determining the amount of radioactivity in these cells. As

shown in Figure 10, the hepatocytes were the major site for the uptake of Gal-PEG-^{33}P-ODN. At 30 min about 58% of the total liver recovery was in the hepatocytes compared to only 30% for the ^{33}P-ODNs (Figure 10). Accordingly, the uptake of Gal-PEG-^{33}P-ODN in the liver nonparantchymal cells (NPC) was 42% compared to 70% for ^{33}P-ODN. This suggests that a large % of the injected Gal-PEG-^{33}P-ODN was taken up by the liver via asialoglycoprotein receptor-mediated endocytosis.

DISCUSSION

Systemic delivery of ODNs is promising for treating both genetic and acquired diseases. Phosphorothioate (PS) ODNs are by far the most extensively studied, and significant progress has been made which resulted in one commercial product (Vitravene) as well as several promising clinical trials (31). To enhance the cellular uptake of ODNs by HepG2.2.15 cells which are stably transfected with hepatitis B virus (HBV), Wu and Wu conjugated asialoorosomucoid to poly (L-lysine) and then formed complex with 21 mer ODN complementary to a portion of human HBV. There was significant increase in ODNs uptake by HepG 2.2.15 cells, and the concentration of Hepatitis B Surface Antigen (HBsAg) was 80% lower than controls after 24 hr (32). However, these authors did not determine the biodistribution of asialooromucoid-PLL/ODN complexes after systemic administration in rodents.

We have previously shown that although complex formation with Gal-PLL enhances ODN uptake by hepatocytes after systemic administration in mice, the difference in the intracellular distribution of Gal-PLL/ODN and ODN was only moderate, possibly because of the non-specific ionic interaction due to polycations (8). Therefore, in this study, we conjugated ODN to Gal-PEG via an acid labile ester linkage of β-thiopropionate, which will be cleaved in response to a pH decrease in the endosome. Oishi et al. (2003) demonstrated the hydrolysis of β-thiopropionate linkage (easter linkage) of the PEG-ODN conjugate at pH 5.5, but not at pH 7.4 even after incubation at 37ºC for 24h (23).

Consistent with our results on Gal-PLL/ODN complexes (8), the plasma kinetic disposition of Gal-PEG-^{33}P-ODN was characterized by rapid distribution to most peripheral tissues, with the highest disposition in the liver (Figures 7A and B). Bioconjugation with Gal-PEG decreased the urinary clearance of ODNs to a great extent (8). The liver accumulation of Gal-PEG-^{33}P-ODN, including radioactivity and ODN concentration, significantly increased within a short time and reached its peak at 30 min post administration. Generally, after the peak time point the accumulation of the radioactivity and the concentration should decrease along the time. However, in the present study both of them showed slight increase in the hepatic uptake at 240min and then decreased, while in other organs the accumulation and concentration of ODNs increased significantly until 24hr. The possible reason for this phenomenon is that after endocytosis of Gal-PEG-ODN by the liver cells the *β*–thiopropionate linkage becomes not stable and ODN will be released from conjugate gradually. The degradation reaction makes the cell an ODN depot. Then some of ODNs can distribute to all over the body.

We determined the role of the asialoglycoprotein receptors on biodistribution of Gal-PEG-^{33}P-ODN in rats by the competition effect of excess Gal-BSA on the hepatic uptake of ODNs. There was significant decrease in ODN deposition to the liver, but increase in its accumulation to other organs and tissues, suggesting that Gal-PEG-ODN was taken up by hepatocytes via the galactose-specific asialoglycoprotein receptor mediated endocytosis (Figure 9). The higher uptake of ODNs in hepatocytes compared with nonparantchymal cells in the cellular distribution (Figure 10) and the highest accumulation of ODNs in liver compared with other organs in whole body level biodistribution after ODN conjugated with Gal-PEG (Figure 7) further confirmed this result.

In conclusion, in this study we synthesized a Gal-PEG-ODN conjugate for site-specific delivery to hepatocytes. In contrast to ^{33}P-ODN, Gal-PEG-^{33}P-ODN was efficiently taken up by hepatocytes and less efficiently by non-parenchymal cells (Figure 10). Thus, non-ionic Gal-PEG-ODN is a promising delivery system which can be used for targeted delivery of ODN or siRNA into hepatocytes to treat various liver diseases associated with hepatocyte injury and inflammation.

Acknowledgements

This work was supported by a grant EB003922 from the NIH. The authors thank Dr. Ying Tu for her help with optimization of HPLC condition.

References

1. Felgner JH, Kumar R, Sridhar CN, Wheeler CJ, Tsai YJ, Border R, Ramsey P, Martin M, Felgner PL. Enhanced gene delivery and mechanism studies with a novel series of cationic lipid formulations. J Biol Chem 1994;269:2550–61. [PubMed: 8300583]
2. Liu F, Yang J, Huang L, Liu D. New cationic lipid formulations for gene transfer. Pharm Res 1996;13:1856–60. [PubMed: 8987084]
3. Mahato RI, Rolland A, Tomlinson E. Cationic lipid-based gene delivery systems: pharmaceutical perspectives. Pharm Res 1997;14:853–9. [PubMed: 9244140]
4. Goula D, Remy JS, Erbacher P, Wasowicz M, Levi G, Abdallah B, Demeneix BA. Size, diffusibility and transfection performance of linear PEI/DNA complexes in the mouse central nervous system. Gene Ther 1998;5:712–7. [PubMed: 9797878]
5. Benns JM, Choi JS, Mahato RI, Park JS, Kim SW. pH-sensitive cationic polymer gene delivery vehicle: N-Ac-poly(L-histidine)-graft-poly(L-lysine) comb shaped polymer. Bioconjug Chem 2000;11:637–45. [PubMed: 10995206]
6. De Smedt SC, Demeester J, Hennink WE. Cationic polymer based gene delivery systems. Pharm Res 2000;17:113–26. [PubMed: 10751024]
7. Mahato RI, Cheng K, Guntaka RV. Modulation of gene expression by antisense and antigene oligodeoxynucleotides and small interfering RNA. Expert Opin Drug Deliv 2005;2:3–28. [PubMed: 16296732]
8. Mahato RI, Takemura S, Akamatsu K, Nishikawa M, Takakura Y, Hashida M. Physicochemical and disposition characteristics of antisense oligonucleotides complexed with glycosylated poly(L-lysine). Biochem Pharmacol 1997;53:887–95. [PubMed: 9113108]
9. Temsamani J, Roskey A, Chaix C, Agrawal S. In vivo metabolic profile of a phosphorothioate oligodeoxyribonucleotide. Antisense Nucleic Acid Drug Dev 1997;7:159–65. [PubMed: 9212906]
10. Graham MJ, Crooke ST, Monteith DK, Cooper SR, Lemonidis KM, Stecker KK, Martin MJ, Crooke RM. In vivo distribution and metabolism of a phosphorothioate oligonucleotide within rat liver after intravenous administration. J Pharmacol Exp Ther 1998;286:447–58. [PubMed: 9655890]
11. Rusckowski M, Qu T, Roskey A, Agrawal S. Biodistribution and metabolism of a mixed backbone oligonucleotide (GEM 231) following single and multiple dose administration in mice. Antisense Nucleic Acid Drug Dev 2000;10:333–45. [PubMed: 11079573]
12. Graham MJ, Crooke ST, Lemonidis KM, Gaus HJ, Templin MV, Crooke RM. Hepatic distribution of a phosphorothioate oligodeoxynucleotide within rodents following intravenous administration. Biochem Pharmacol 2001;62:297–306. [PubMed: 11434902]
13. Staud F, Nishikawa M, Takakura Y, Hashida M. Liver uptake and hepato-biliary transfer of galactosylated proteins in rats are determined by the extent of galactosylation. Biochim Biophys Acta 1999;1427:183–92. [PubMed: 10216235]
14. Attie AD, Pittman RC, Steinberg D. Metabolism of native and of lactosylated human low density lipoprotein: evidence for two pathways for catabolism of exogenous proteins in rat hepatocytes. Proc Natl Acad Sci U S A 1980;77:5923–7. [PubMed: 6160586]

15. Biessen EA, Beuting DM, Vietsch H, Bijsterbosch MK, Van Berkel TJ. Specific targeting of the antiviral drug 5-iodo 2′-deoxyuridine to the parenchymal liver cell using lactosylated poly-L-lysine. J Hepatol 1994;21:806–15. [PubMed: 7890898]

16. Ye Z, Cheng K, Guntaka RV, Mahato RI. Receptor-mediated hepatic uptake of M6P-BSA-conjugated triplex-forming oligonucleotides in rats. Bioconjug Chem 2006;17:823–30. [PubMed: 16704223]

17. Rajur SB, Roth CM, Morgan JR, Yarmush ML. Covalent protein-oligonucleotide conjugates for efficient delivery of antisense molecules. Bioconjug Chem 1997;8:935–40. [PubMed: 9404669]

18. Healy JM, Lewis SD, Kurz M, Boomer RM, Thompson KM, Wilson C, McCauley TG. Pharmacokinetics and biodistribution of novel aptamer compositions. Pharm Res 2004;21:2234–46. [PubMed: 15648255]

19. Zhao H, Greenwald RB, Reddy P, Xia J, Peng P. A new platform for oligonucleotide delivery utilizing the PEG prodrug approach. Bioconjug Chem 2005;16:758–66. [PubMed: 16029016]

20. Zhao H, Peng P, Longley C, Zhang Y, Borowski V, Mehlig M, Reddy P, Xia J, Borchard G, Lipman J, Benimetskaya L, Stein CA. Delivery of G3139 using releasable PEG-linkers: impact on pharmacokinetic profile and anti-tumor efficacy. J Control Release 2007;119:143–52. [PubMed: 17397960]

21. Bonora GM, Ivanova E, Zarytova V, Burcovich B, Veronese FM. Synthesis and characterization of high-molecular mass polyethylene glycol-conjugated oligonucleotides. Bioconjug Chem 1997;8:793–7. [PubMed: 9404651]

22. Oishi M, Nagasaki Y, Itaka K, Nishiyama N, Kataoka K. Lactosylated poly(ethylene glycol)-siRNA conjugate through acid-labile beta-thiopropionate linkage to construct pH-sensitive polyion complex micelles achieving enhanced gene silencing in hepatoma cells. J Am Chem Soc 2005;127:1624–5. [PubMed: 15700981]

23. Oishi M, Sasaki S, Nagasaki Y, Kataoka K. pH-responsive oligodeoxynucleotide (ODN)-poly (ethylene glycol) conjugate through acid-labile beta-thiopropionate linkage: preparation and polyion complex micelle formation. Biomacromolecules 2003;4:1426–32. [PubMed: 12959615]

24. Cheng K, Ye Z, Guntaka RV, Mahato RI. Biodistribution and hepatic uptake of triplex-forming oligonucleotides against type alpha1(I) collagen gene promoter in normal and fibrotic rats. Mol Pharm 2005;2:206–17. [PubMed: 15934781]

25. Guicciardi ME, Gores GJ. Apoptosis: a mechanism of acute and chronic liver injury. Gut 2005;54:1024–33. [PubMed: 15951554]

26. Monsigny M, Roche AC, Midoux P. Uptake of neoglycoproteins via membrane lectin(s) of L1210 cells evidenced by quantitative flow cytofluorometry and drug targeting. Biol Cell 1984;51:187–96. [PubMed: 6240301]

27. Sando GN, Karson EM. p-Isothiocyanatophenyl 6-phospho-alpha-D-mannopyranoside coupled to albumin. A model compound recognized by the fibroblast lysosomal enzyme uptake system. 1. Chemical synthesis and characterization. Biochemistry 1980;19:3850–5. [PubMed: 7190837]

28. Monsigny M, Petit C, Roche AC. Colorimetric determination of neutral sugars by a resorcinol sulfuric acid micromethod. Anal Biochem 1988;175:525–30. [PubMed: 3239778]

29. Hendriks HF, Brouwer A, Knook DL. Isolation, purification, and characterization of liver cell types. Methods Enzymol 1990;190:49–58. [PubMed: 1965003]

30. Terada T, Nishikawa M, Yamashita F, Hashida M. Analysis of the molecular interaction of glycosylated proteins with rabbit liver asialoglycoprotein receptors using surface plasmon resonance spectroscopy. J Pharm Biomed Anal 2006;41:966–72. [PubMed: 16546339]

31. Orr RM, Dorr FA. Clinical studies of antisense oligonucleotides for cancer therapy. Methods Mol Med 2005;106:85–111. [PubMed: 15375314]

32. Wu GY, Wu CH. Specific inhibition of hepatitis B viral gene expression in vitro by targeted antisense oligonucleotides. J Biol Chem 1992;267:12436–9. [PubMed: 1618751]

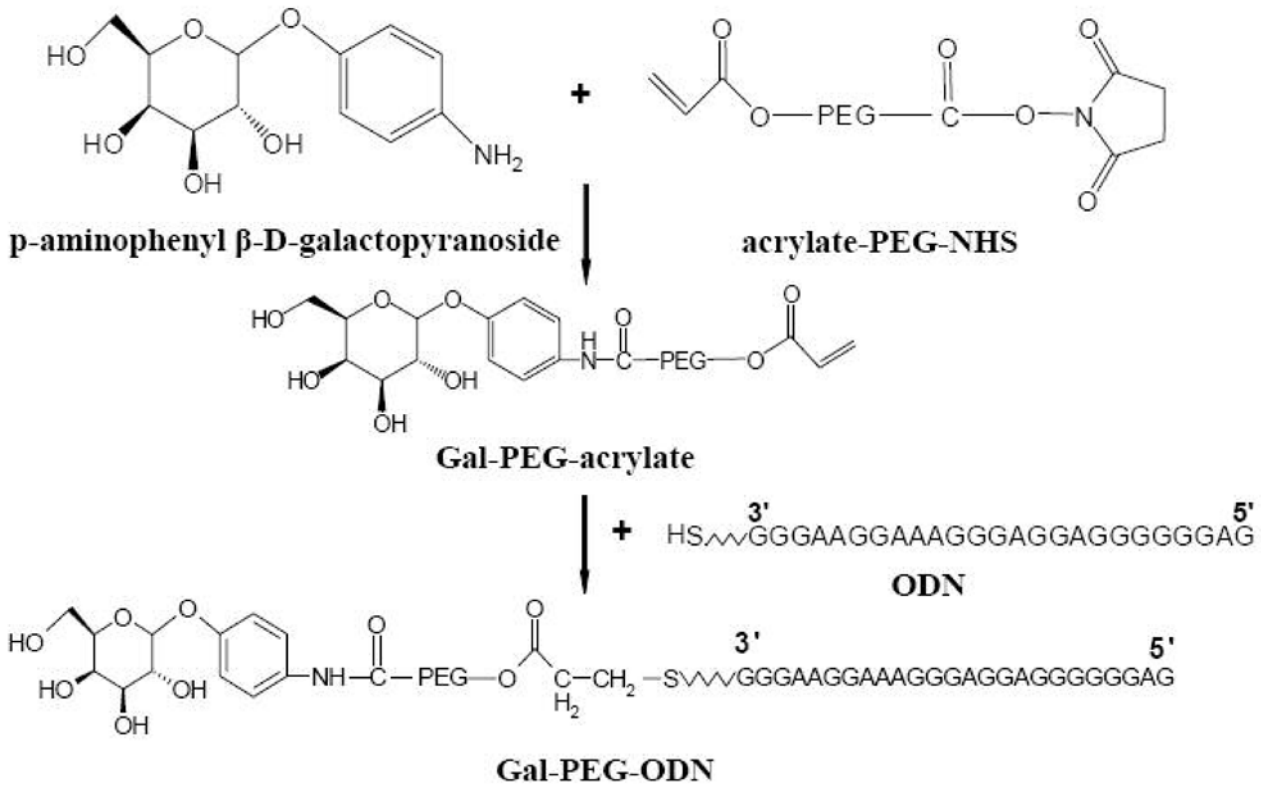

Figure 1.

Synthesis scheme of Gal-PEG-ODN. p-Nitrophenyl β-D-galactopyranoside was reduced to p-aminophenyl β-D-galactopyranoside and then conjugated to 3′-thiol ODN by Michael addition.

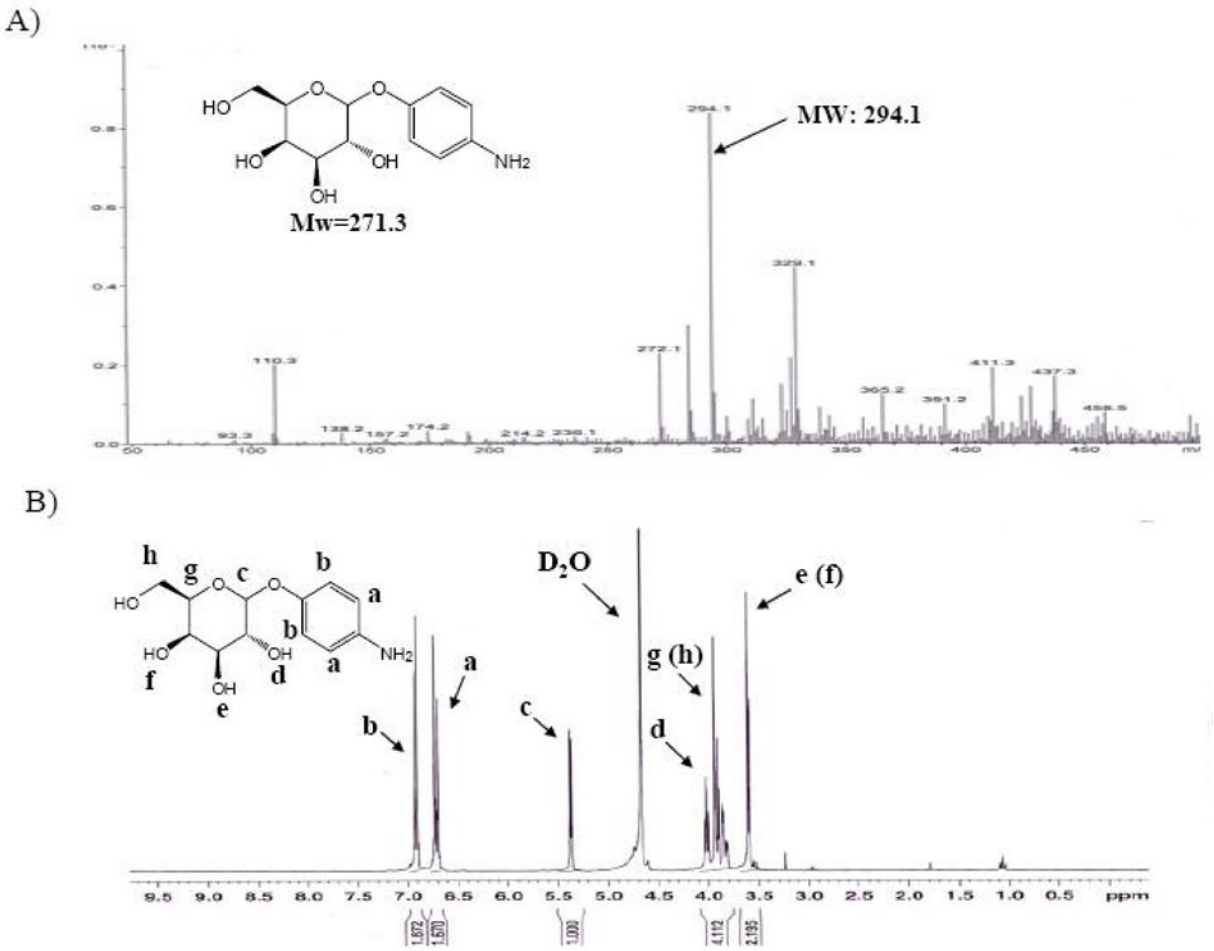

Figure 2.

Characterization of p-aminophenyl β-D-galactopyranoside with electron spry ionization mass spectrometry (ESI-MS) and ^{1}H-NMR. A) Electron spray ionization mass spectra were obtained after dissolving the product in methanol on an ESQUIRE-LC Ion Trap LC/MS system. B) For ^{1}H NMR, samples were dissolved in D_2O and the spectra were recorded on a Bruker ARX-300 MHz NMR spectrometer at 25 °C.

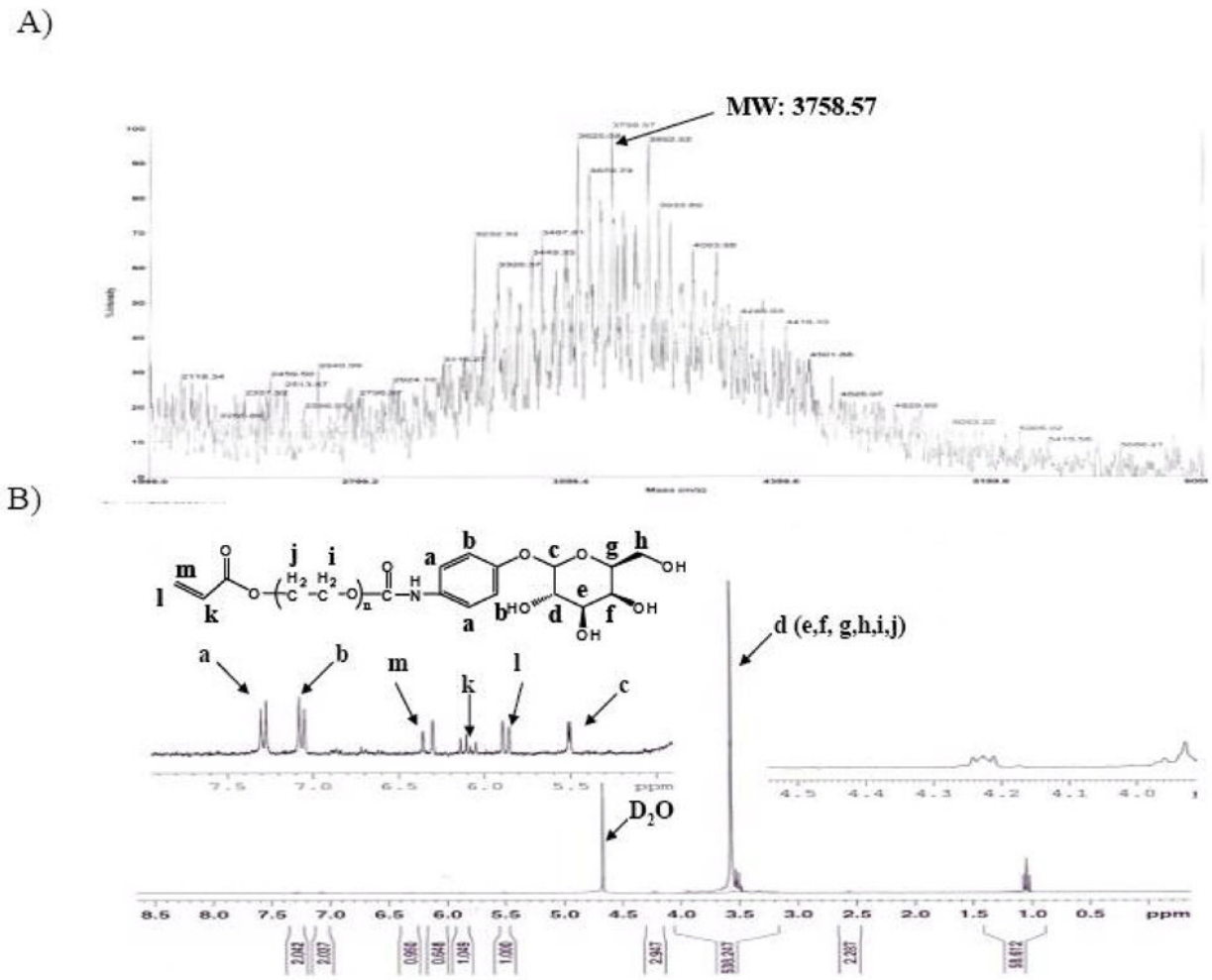

Figure 3.

Characterization of Gal-PEG-acrylate with MALDI-TOF-MS and ^{1}H-NMR. A) In MALDI-TOF-MS the ratio between Gal-PEG-acrylate and DHB was 1:2. The spectrum was recorded on Voyager-DE RP (PerSeptive Biosystems Inc., MA). B) For ^{1}H NMR, samples were dissolved in D_2O and the spectra were recorded on a Bruker ARX-300 MHz NMR spectrophotometer at 25 °C.

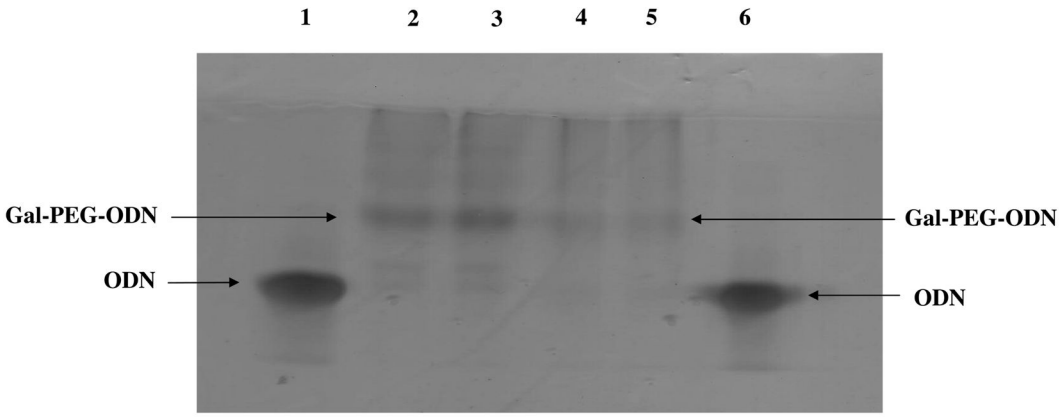

Figure 4.

Identification of Gal-PEG-ODN by polyacrylamide gel electrophoresis (PAGE) at 80v for 100min, followed by staining with methylene blue for one night. Lane 1 and 6: ODN 2μg; lane 2 and 3: Gal-PEG-ODN 2μg; lane 4 and 5: Gal-PEG-ODN 1μg.

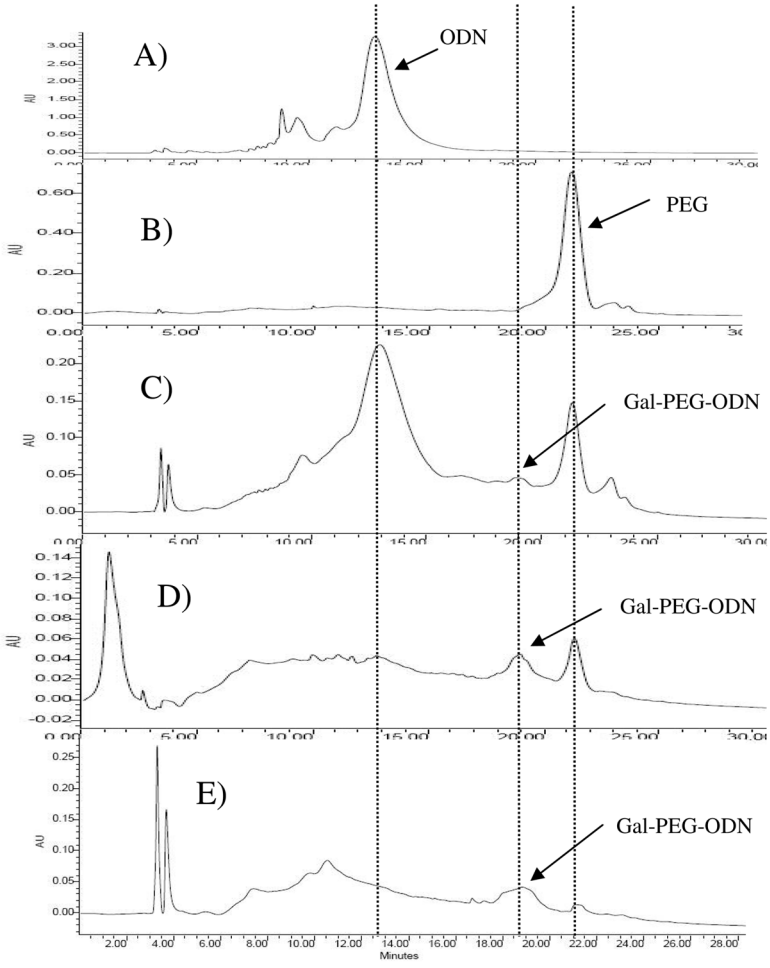

Figure 5.
HPLC chromatograms of (A) ODN, (B) PEG, (C) reaction mixture, (D) during purification and (E) after purification of Gal-PEG-ODN.

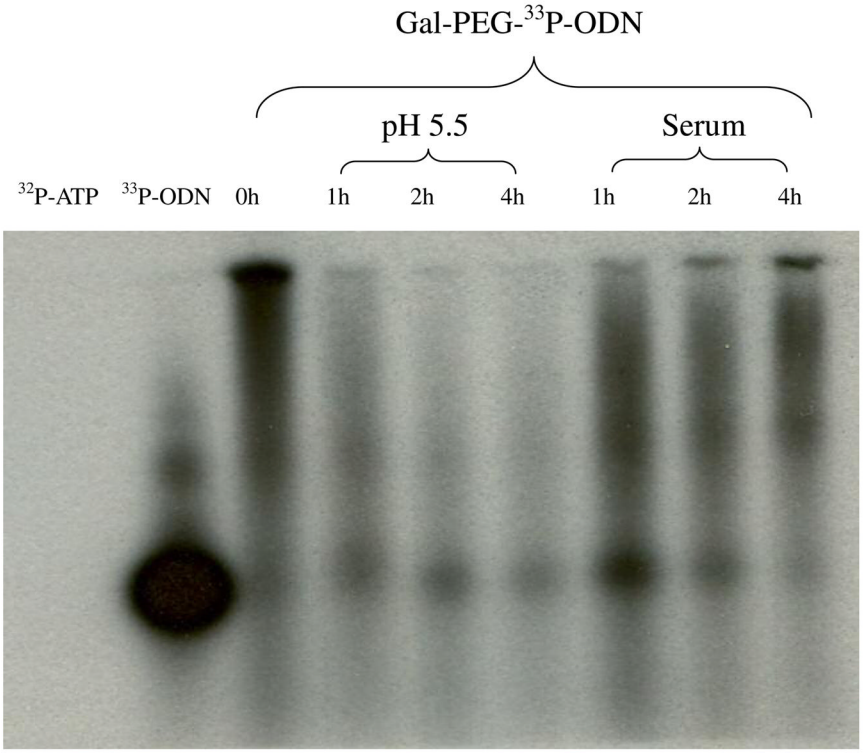

Figure 6.

Dissociation and stability study of Gal-PEG-^{33}P-ODN. Dissociation of ^{33}P-ODN from Gal-PEG-^{33}P-ODN was determined by incubating the conjugate at 37ºC in pH 5.5 buffer, while its stability was determined by incubating the conjugate at 37ºC in rat serum. The band for Gal-PEG-^{33}P-ODN decrease with time when incubate at acidic pH.

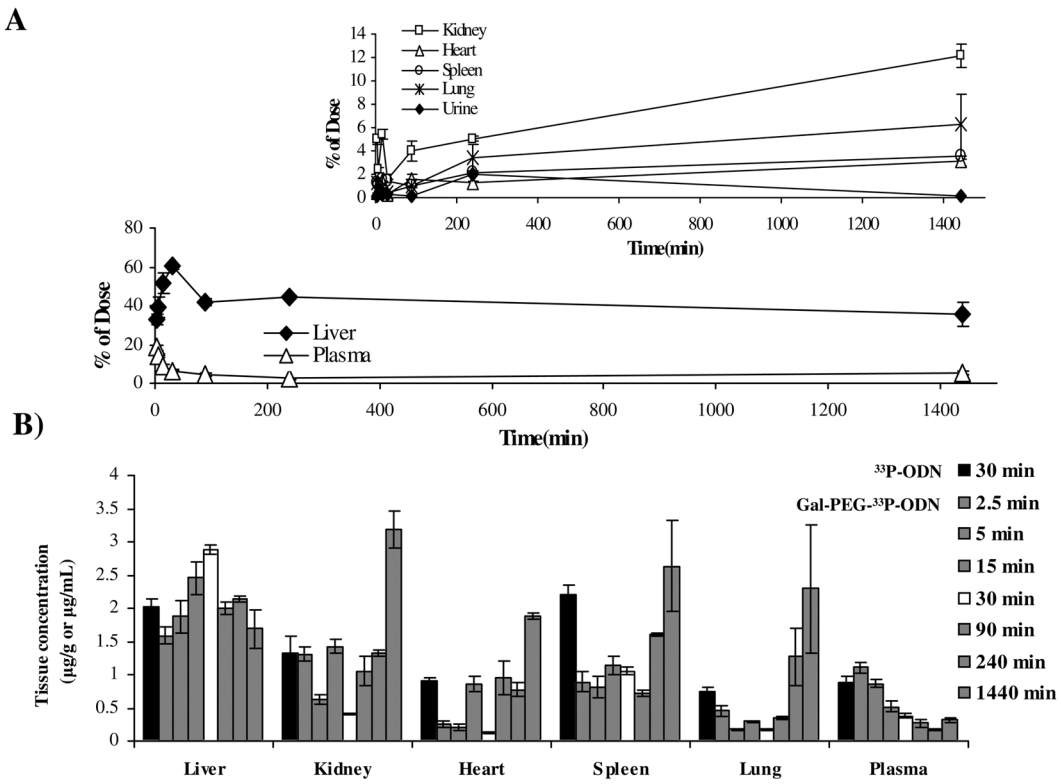

Figure 7.

Accumulation (A) and concentration (B) of Gal-PEG-^{33}P-ODN after tail vein injection into rats at a dose of 0.2mg ODN/Kg of body weight. To compare the biodistribution profiles of Gal-PEG-^{33}P-ODN, ^{33}P-ODN was also injected, and ODN accumulation and concentration in different tissues were determined at 30min post-injection. Following blood collection by cardiac puncture and urine collection from the bladder, the tissues were isolated, digested and subjected to radioactivity measurement. Results are presented as the mean ± S.D. (n=4).

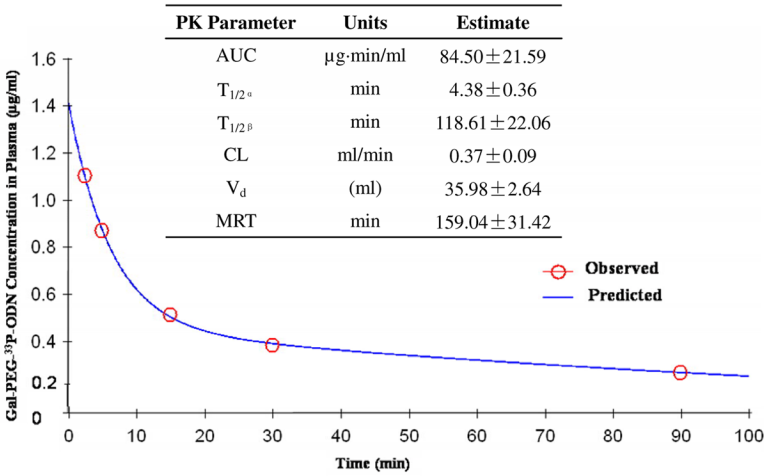

Figure 8.

Plasma data was analyzed using a two compartment model with WinNonlin Professional (version 5.0.1) software. Data are represented as the mean ± SD (n=4).

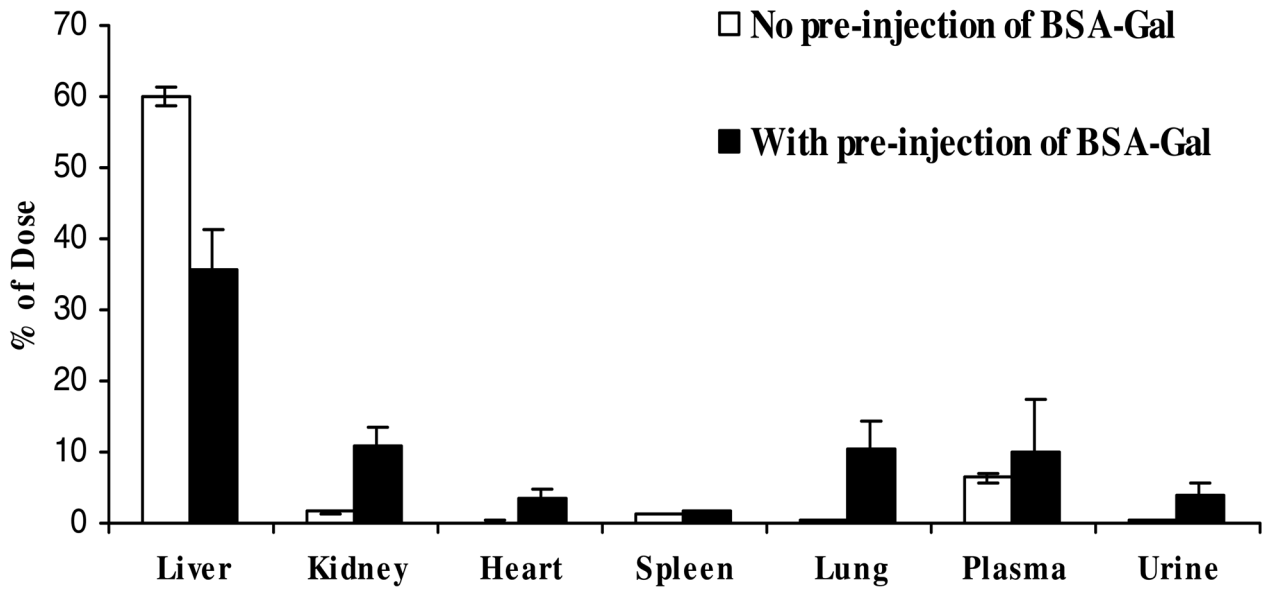

Figure 9.

Effect of Gal-BSA on biodistribution of Gal-PEG-^{33}P-ODN after systemic administration into rats. Gal-BSA (10mg/Kg) was injected intravenously into rats 2 minutes before the injection of Gal-PEG-^{33}P-ODN at a dose of 0.2 mg/Kg. At 30 minute post injection, rats were sacrificed, major organs were isolated and radioactivity was determined. Values are the mean ± S.D. of 4 rats.

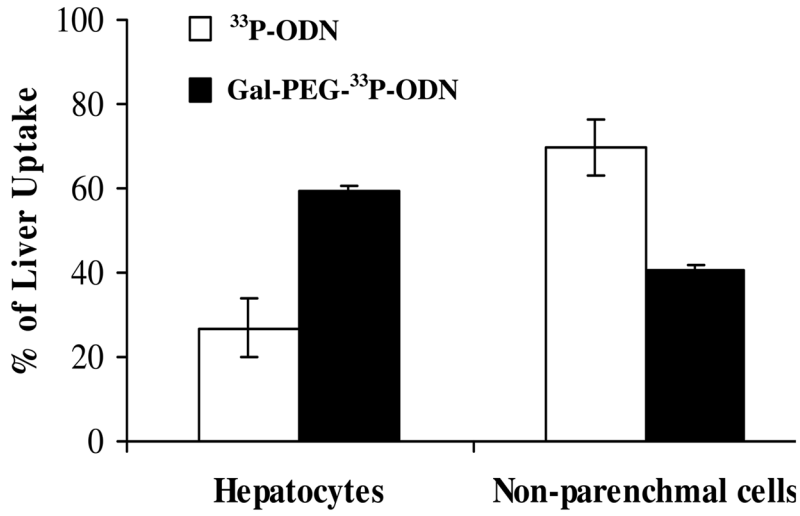

Figure 10.

Hepatic cellular localization of ^{33}P-ODN and Gal-PEG-^{33}P-ODNs. The liver was perfused by collagenase/pronase digestion at 30 min post injection of ^{33}P-ODN or Gal-PEG-^{33}P-ODN at a dose of 0.2 mg/Kg. Parenchymal and non-parenchymal cells were separated and the associated radioactivity was measured. Values are the mean ± S.D. of 4 rats.

Table 1

Tissue uptake rate index and clearance of ^{33}P-ODN and Gal-PEG-^{33}P-ODN systemic administration into rats

	AUC (μg-min/ml)	Tissue uptake rate index (μL · h^{-1} · g^{-1})					Organ clearance (μL · $^{-1}$)				
		Liver	Kidney	Heart	Spleen	Lung	Liver	Kidney	Heart	Spleen	Lung
	95.15 ± 5.11	376.15 ± 38.34	235.23 ± 29.19	48.76 ± 3.42	204.73 ± 9.64	55.23 ± 8.90	2218.09 ± 208.56	241.00 ± 41.08	22.96 ± 1.94	82.86 ± 7.35	42.21 ± 8.44
^{33}P ODN	84.50 ± 21.59	2663.27 ± 56.63	376.56 ± 11.16	119.24 ± 10.81	969.26 ± 51.79	161.16 ± 7.00	16674.22 ± 354.55	428.81 ± 12.71	59.67 ± 5.41	395.84 ± 21.15	131.22 ± 5.70